



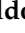




Article

Enhancing the Wear Performance of 316L Stainless Steel with Nb₂O₅ Coatings Deposited via DC Sputtering at Room Temperature under Varied Environmental Conditions

Murilo Oliveira Alves Ferreira ^{1,*}, Victor Auricchio Fernandes Morgado ¹, Kauê Ribeiro dos Santos ¹, Rogério Valentim Gelamo ², Fábio Edson Mariani ³, Natália Bueno Leite Slade ⁴, Mateus Mota Morais ⁵, Carlos Alberto Fortulan ⁵, Rodrigo Galo ⁶, Renato Goulart Jasinevicius ⁵, Haroldo Cavalcanti Pinto ¹ and Jéferson Aparecido Moreto ^{1,*}

- ¹ Materials Engineering Department, São Carlos School of Engineering, University of São Paulo (USP), São Carlos 13563-120, SP, Brazil; victor.auricchio@usp.br (V.A.F.M.); kauesantos@usp.br (K.R.d.S.); haroldo@sc.usp.br (H.C.P.)
- ² Institute of Technological and Exact Sciences, Federal University of Triângulo Mineiro (UFTM), Uberaba 38064-200, MG, Brazil; rogelamo@gmail.com
- ³ Department of Production Engineering, São Carlos School of Engineering, University of São Paulo (USP), São Carlos 13566-590, SP, Brazil; mariani.fabio@usp.br
- ⁴ Institute of Exact Sciences, Naturals and Education, Federal University of Triângulo Mineiro (UFTM), Uberaba 38064-200, MG, Brazil; natalia.slade@uftm.edu.br
- ⁵ Mechanical Engineering Department, São Carlos School of Engineering, University of São Paulo (USP), São Carlos 13566-590, SP, Brazil; mateus.morais@usp.br (M.M.M.); fortulan@usp.br (C.A.F.); renatogj@sc.usp.br (R.G.J.)
- ⁶ School of Dentistry of Ribeirão Preto, University of São Paulo (USP), Ribeirão Preto 14040-904, SP, Brazil; rogalof@forp.usp.br
- * Correspondence: moaferreira@usp.br (M.O.A.F.); jamoreto@usp.br (J.A.M.)



Citation: Ferreira, M.O.A.; Morgado, V.A.F.; dos Santos, K.R.; Gelamo, R.V.; Mariani, F.E.; Slade, N.B.L.; Morais, M.M.; Fortulan, C.A.; Galo, R.; Jasinevicius, R.G.; et al. Enhancing the Wear Performance of 316L Stainless Steel with Nb₂O₅ Coatings Deposited via DC Sputtering at Room Temperature under Varied Environmental Conditions. *Lubricants* **2024**, *12*, 345. <https://doi.org/10.3390/lubricants12100345>

Received: 6 September 2024

Revised: 2 October 2024

Accepted: 4 October 2024

Published: 6 October 2024



Copyright: © 2024 by the authors. Licensee MDPI, Basel, Switzerland. This article is an open access article distributed under the terms and conditions of the Creative Commons Attribution (CC BY) license (<https://creativecommons.org/licenses/by/4.0/>).

Abstract: Niobium-based oxides have garnered increased attention in recent years for their remarkable enhancement of corrosion resistance, as well as biofunctional properties of various metallic materials, including 316L SS. However, the mechanical properties of these promising coatings have not been fully elucidated. This study investigated how much the environmental conditions (air, artificial saliva, and NaCl solution) impact the wear performance of 316L SS without and with Nb₂O₅ coatings deposited via the reactive sputtering technique. The results exhibited a notable decrease in friction coefficient (55% in air, 18% in artificial saliva, 10% in 0.9 wt% NaCl solution), wear area (46% in air, 36% in AS, 17.5% in 0.9 wt% NaCl solution), and wear rate (44.0% in air, 19.5% in AS, 12.0% in 0.9 wt% NaCl solution). Ultimately, the results obtained in the present study elucidate the synergistic mechanisms of corrosion and wear in 316L SS containing Nb₂O₅ coatings, highlighting its significant potential for applications in the biomedical sector.

Keywords: 316L SS; sputtering; niobium films; wear resistance

1. Introduction

With advancements in various medical fields and the subsequent rise in life expectancy, the demand for innovative biomaterials has become paramount [1]. For instance, the number of hip and knee replacement surgeries continues to rise significantly each year [2]. However, the materials currently employed in these procedures have significant drawbacks for many patients, including implant loosening, infections, and, in the case of Ti-6Al-4V alloy, the potential release of harmful metal ions over time [3–8]. Recently, 316L stainless steel (316 L SS) has garnered increased attention as an implantable biomaterial due to its cost-effectiveness compared to titanium-based alloys, and its relatively high biocompatibility [9–15]. Despite these advantages, 316L SS has certain limitations, particularly in

terms of corrosion resistance and wear performance when exposed to the highly aggressive conditions of the human body [5].

The surface functionalisation of 316L SS with niobium-based coatings, employing the reactive sputtering technique, has emerged as a highly effective alternative for improving corrosion resistance and enhancing biological response across various alloy types [16–27]. The earlier studies conducted by this research group [26,27] highlighted the significant influence of Nb₂O₅ thin films on the wear properties of Ti-6Al-4V alloy. The authors observed an impressive 80% reduction in the wear volume of the coated material compared to the uncoated alloy. Moreto and colleagues [27] investigated the effect of Nb₂O₅ on the biological response of 316L SS and demonstrated that the coating not only improved protection in a physiological environment, but also reduced toxicity, leading to a lower inflammatory response compared to the uncoated specimens. Ferreira et al. [26] evaluated the electrochemical behaviour of 316L SS coated with Nb₂O₅ and amorphous carbon thin films in a 0.6 mol L⁻¹ NaCl solution. Their assessment included the use of open circuit potential (OCP), potentiodynamic polarisation curves (PPCs), and electrochemical impedance spectroscopy (EIS). As reported by the authors [26], the findings indicated that the surface treatments significantly improved the corrosion resistance of 316L SS, since the coatings acted as effective protective barriers, mitigating uniform and localised corrosion processes that could compromise the integrity of the substrate.

In this context, Nb₂O₅-based coatings present a promising strategy for extending the lifespan of biomedical implants. Given the significant gap in the international literature regarding studies that focus on wear testing of Nb₂O₅ coatings, it is essential to advance research in this area. The present work is an innovative applied research initiative aimed at exploring the impact of various environmental conditions on the wear performance of Nb₂O₅ coatings deposited on 316L SS surfaces by using the reactive sputtering technique. To accomplish this, a series of wear tests were conducted using a pin-on-disk apparatus under various environmental conditions, including air, 0.9 wt% NaCl solution, and artificial saliva (AS). It is important to emphasise that, following the mechanical tests, a comprehensive morphological analysis was conducted to elucidate the wear mechanisms.

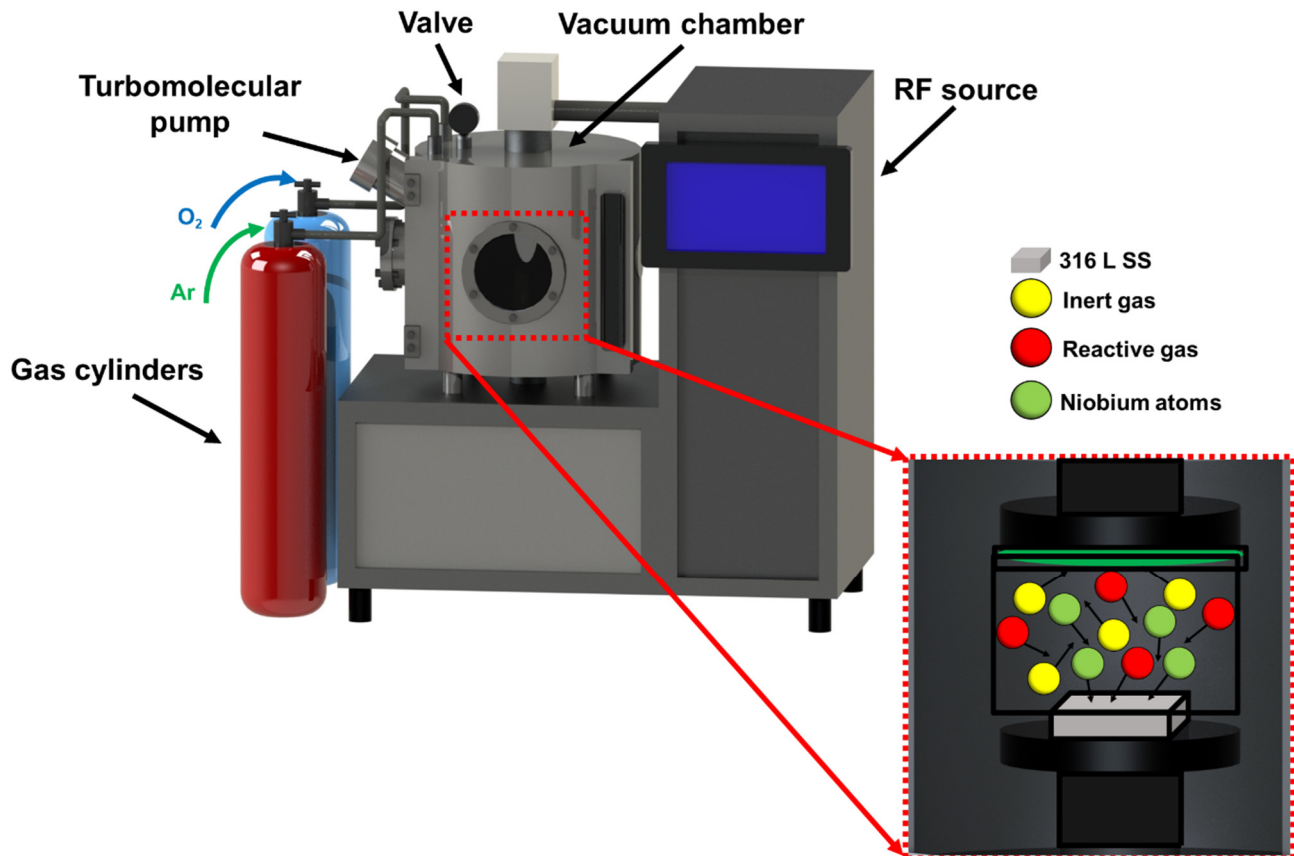
2. Materials and Methods

2.1. Materials

Square plate samples (20 mm × 20 mm × 2 mm) of 316L SS were obtained through electrical erosion cutting and subsequently underwent a grinding process using SiC abrasives in the sequence range 800, 1200, 2400, and 4000 mesh. Polishing was then performed using 3, 2, and 1 μm diamond pastes and an ultrasonic bath for 10 min each in distilled water and isopropyl alcohol. The chemical composition (wt%) of the 316L SS was previously validated by this research group in previously published work [6], and is presented on Table 1. As reported in the literature, the hardness of the 316L SS is about 95 HRB [28]. To deposit niobium-based coatings on the 316L SS surfaces, a DC-magnetron sputtering chamber was used (see Figure 1), featuring 2-inch diameter targets of niobium (99.99%) at a temperature of 25 ± 1 °C. The chamber atmosphere comprised an argon (99.99%) and oxygen (99.99%) mixture at 5.0 and 0.5 mTorr, respectively, with an applied voltage of 440 V and a current of 140 mA. The coating was applied uniformly across the entire surface of the 316L SS specimens. The mechanism of sputtering deposition comprises several steps: (i) plasma formation; (ii) ion bombardment; (iii) ejection of target atoms; (iv) transport of ejected atoms; and (v) film growth on the substrate. During sputtering deposition, various interaction mechanisms can occur among the atoms, gas species, and the substrate surface. Such interactions significantly influence the quality and characteristics of the thin film. By controlling these mechanisms, one can adjust deposition parameters (e.g., substrate temperature, target power, gas pressure), thereby improving the properties and quality of the resulting film. The attractive results of the Nb₂O₅ thin films produced in the present study were achievable solely through the optimisation of the deposition process.

Table 1. Chemical composition of the 316L SS obtained by EDX analysis.

Elements	Cr	Ni	Mo	Mn	Si	Fe
wt%	17.4	9.8	2.5	1.6	0.5	68.2

**Figure 1.** Schematic representation of the experimental apparatus employed to produce Nb₂O₅ coatings on the surfaces of 316L SS by using the reactive sputtering technique.

The fitting of the Nb 3D levels revealed a single phase of Nb₂O₅, which is supported by the predominant contribution at 530.7 eV attributed to O 1s. The DRX results, both measured and Rietveld refined, confirmed the presence of 89 ± 1 wt% Nb₂O₅, 9 ± 1 wt% NbO₂, and 2.1 ± 1 wt% NbO crystalline phases. The oxide compositions were identified using the crystallographic data files PDF 01-089-6902 for NbO, PDF 01-076-1095 for NbO₂, and PDF 01-080-2493 for Nb₂O₅ [26,27,29–31]. By employing these comprehensive datasets, it was possible to identify and confirm the presence of the various niobium oxides, which play a crucial role in determining the material properties and functionalities in applications such as coatings. These results are consistent with another study we recently published, where the X-ray absorption near-edge structure spectroscopy (GE-XANES) technique indicated the formation of a uniform layer of Nb₂O₅ thin films on the Ti-6Al-4V alloy surface [32]. Moreover, when combined with a detector such as pnCCD, this approach enables the monitoring of oxidation processes, which, in fact, allows for the identification of the Nb₂O₅ coatings. By integrating grazing exit X-ray fluorescence spectroscopy (GE-XRF) geometry with a pnCCD detector, we offer a scanning-free, nondestructive analysis that is depth-resolved within a sub-micrometer range. The pnCCD detector is distinguished by its capacity to discriminate between various energy levels, thereby enabling the selective analysis of specific emission lines and enhancing the accuracy and precision of our data interpretation [32]. Finally, the Nb₂O₅ thickness of the deposited coating on the 316L SS surface was determined using the atomic force microscopy (AFM) technique.

2.2. Tribological Testing

The wear analysis was conducted using a pin-on-disk tribometer in accordance with ASTM G99-23 standard [33]. All the wear tests were conducted in triplicate maintaining a constant load (5 N), a track diameter of 9 mm, for a period of 300 s, a sliding velocity of 0.01 m s^{-1} and using an alumina sphere (Al_2O_3) with a diameter (\varnothing) 4.78 mm. It is important to emphasise that all wear tests were conducted at a controlled temperature of $25 \pm 1 \text{ }^\circ\text{C}$. The samples were fixed on the disk plate by using an appropriated double-side tape that avoided position changing and unevenness of the samples during the wear tests. Both coated and uncoated samples were tested under three environmental conditions: air, after immersion in 0.9 wt% NaCl solution, and in AS with a neutral pH, free from odor or color. Following the wear tests, both coated and uncoated samples for the three environments were verified using a field emission scanning electron microscope (FEG-SEM) JEOL 7001F, equipped with an Oxford light element detector for energy dispersive X-ray spectroscopy (EDX). The use of both techniques was essential for characterizing the wear track profile on the sample surfaces, enabling the investigation of the wear mechanisms associated with the different conditions. In a collaborative effort, an LEXT model OSL4100 3D confocal laser scanning microscope (CLSM) was employed to examine the topography of the wear track and to obtain information regarding the worn area. To this end, a wear profile assessment was conducted at various points along the track, allowing the determination of the average wear area values. In addition, the wear topography was carried out by using a VEECO non-contact high-resolution profiler Wyko NT 1100. The objective lens used was $20\times$ with field of view lens of $0.5\times$. The measuring technique used was vertical scanning interferometry. The vertical resolution was $<1 \text{ \AA}$ Ra and the lateral spatial sampling was 0.08 to 13.1 mm. The scanning areas for all measurements were kept constant at $470 \mu\text{m} \times 620 \mu\text{m}$. Four measurements were obtained at each 90° around the worn tracks, and average and standard deviation were calculated. Figure 2 presents a schematic illustration of the pin-on-disk apparatus employed in the wear tests, along with its components: the sphere support, load cell, sample holder, arm, applied load, and the disk.

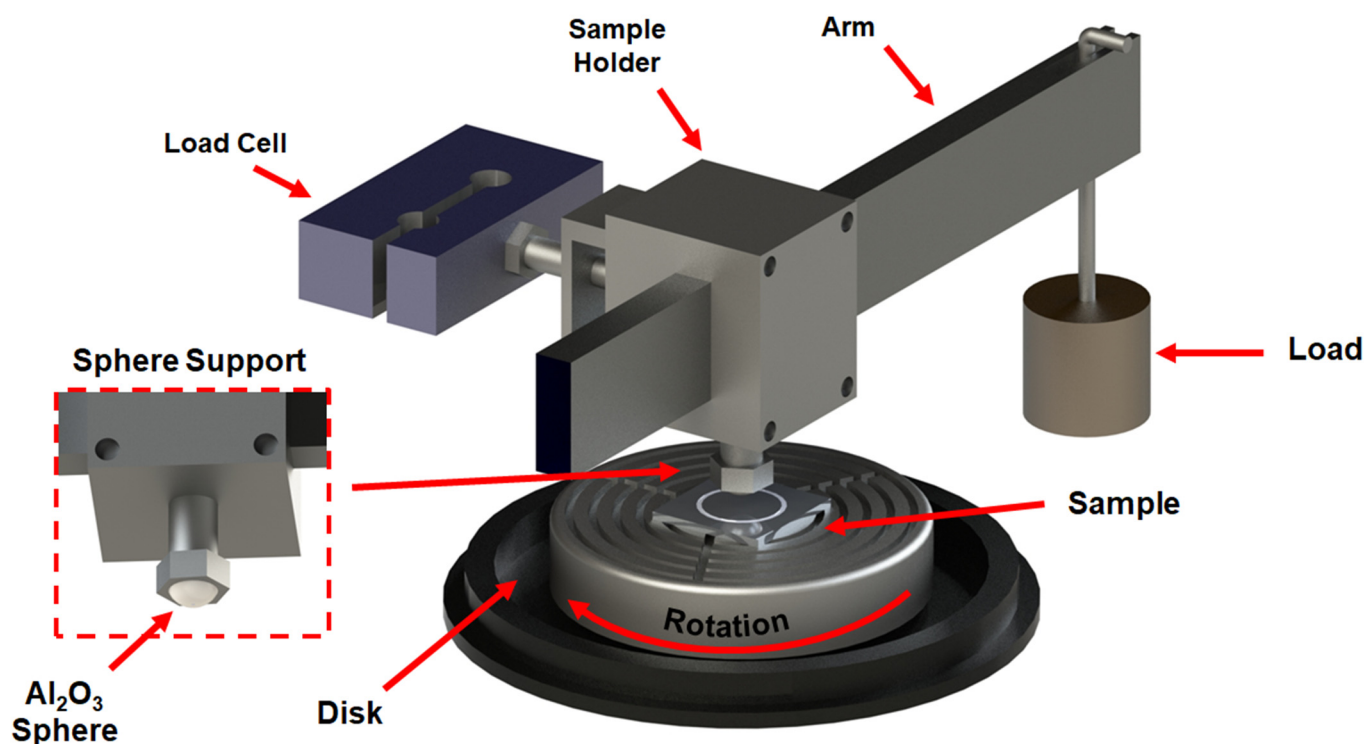


Figure 2. Schematic illustration of the pin-on-disk setup used for the wear tests.

3. Results and Discussion

Both 2D and 3D topographic images of the 316L SS can be seen in Figures 3a and 3b, respectively. In both images, the presence of scratches resulting from the sample grinding process can be observed. The topography of the 316L SS alloy containing Nb_2O_5 coating was evaluated using atomic force microscopy (AFM) over an area of $2.0 \times 2.0 \mu\text{m}$, as illustrated in Figure 4a. The three-dimensional (3D) morphological projection of the 316L SS/ Nb_2O_5 is shown in Figure 4b, while the measurements conducted to determine the thickness of the coating are presented in Figure 4c. It is evident that the Nb_2O_5 thin film was deposited uniformly on the substrate surface, exhibiting the presence of certain grains typically associated with the initial stage of nucleation in the vapour phase. The coating produced in the present work using the reactive sputtering technique exhibits a thickness of approximately 130 nm, and is expected to substantially contribute to enhancing the wear resistance of the 316L SS, as will be discussed in the following sections.

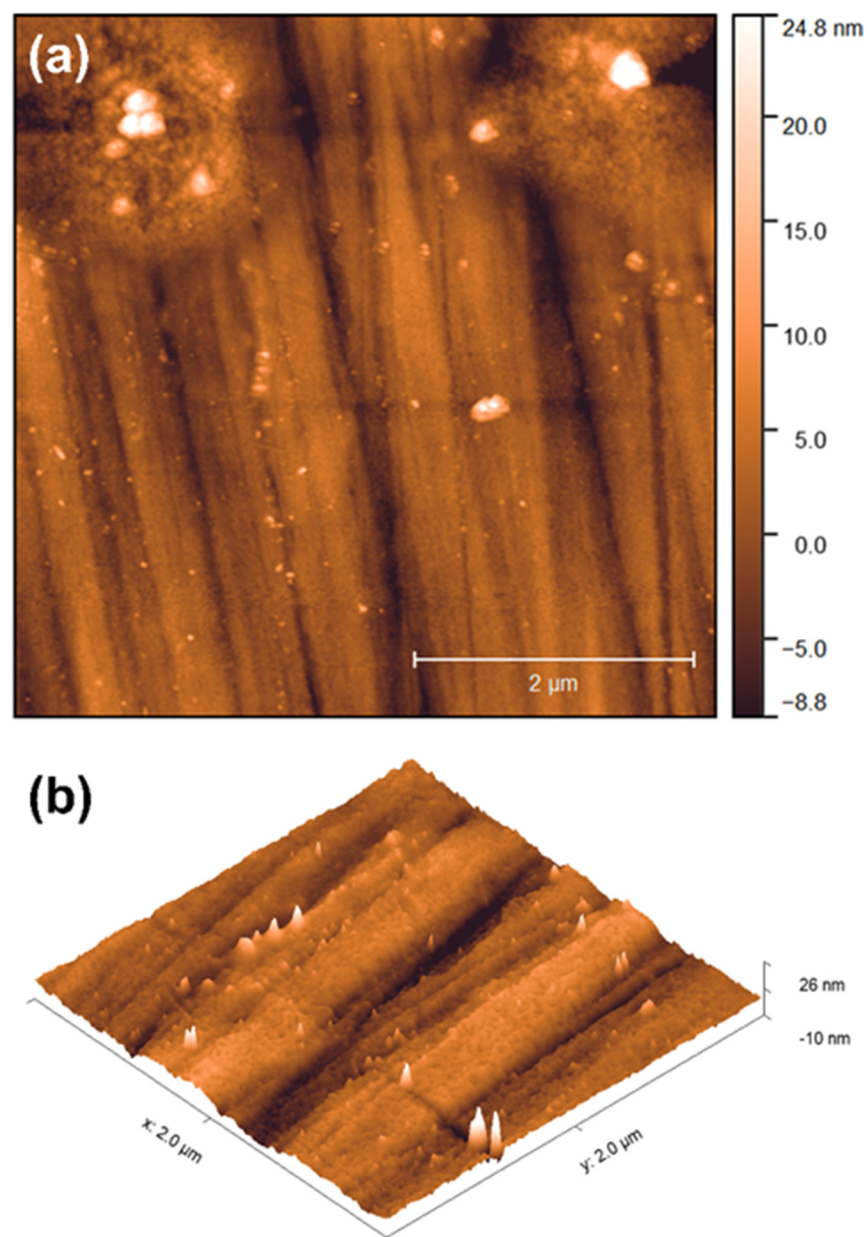


Figure 3. (a) 2D and (b) 3D topographic images of 316L SS, scale $2.0 \mu\text{m} \times 2.0 \mu\text{m}$.

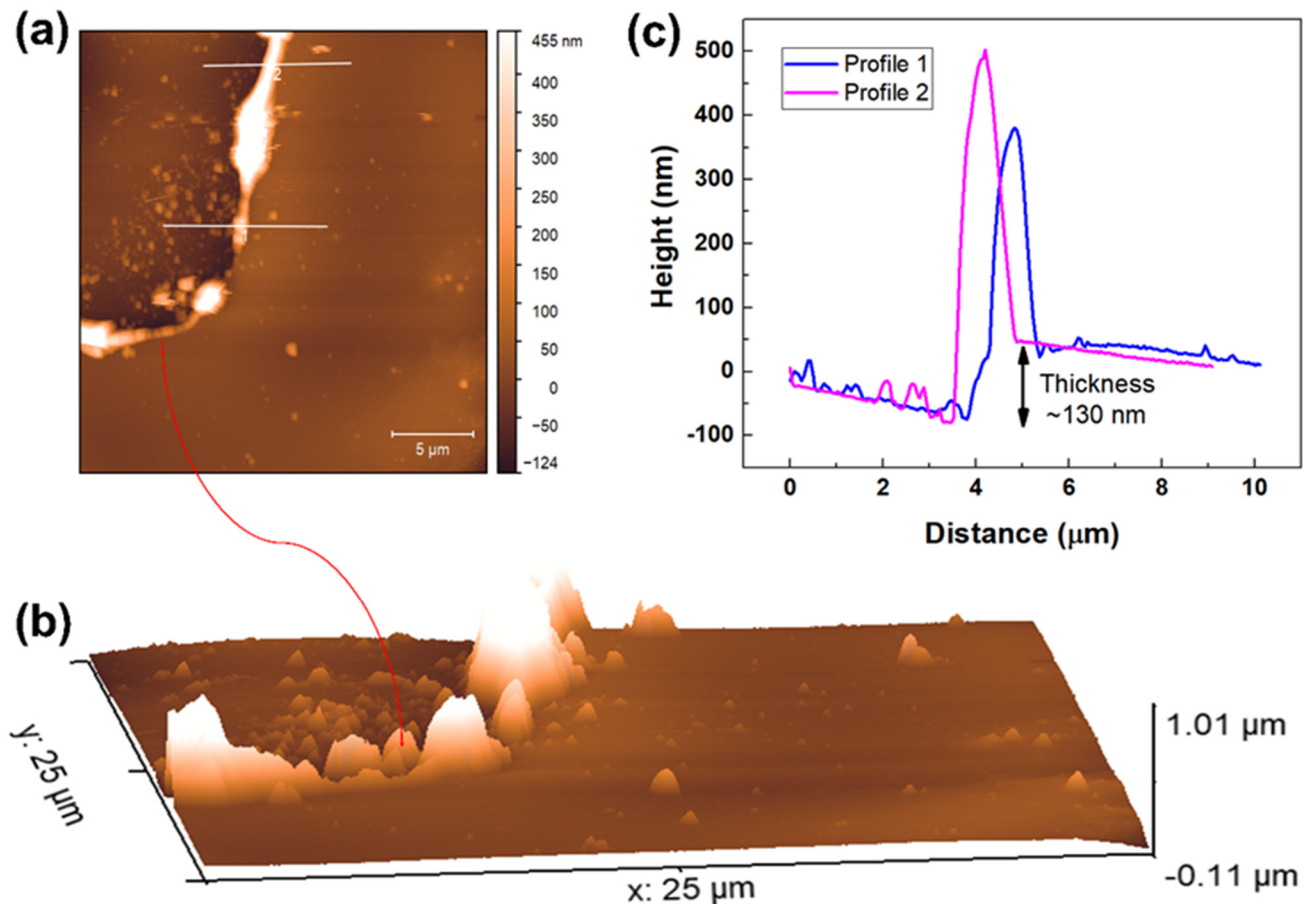


Figure 4. (a) 2D and (b) 3D topographic images of 316L SS containing Nb₂O₅ thin film produced via reactive sputtering technique, and (c) the profilometer values in two regions indicated by traces 1 and 2 in (a).

Figure 5 presents the results of the pin-on-disk analysis, depicting the coefficients of friction (COF) over time. When analysed in air, it was found that the 316L SS exhibited significant COF variation, fluctuating around 0.42. This fluctuation is attributed to the contact of the Al₂O₃ sphere with the non-uniform surface of the sample [34]. However, when the 316L SS/Nb₂O₅ sample is examined, there is a significant reduction in the COF (0.19), with less variation observed from the start of the measurement up to 150 s. The COF of the 316L SS/Nb₂O₅ sample is also significantly lower than that of the uncoated sample. After 150 s, the COF values gradually increase until they reach levels comparable to those of the 316L SS sample. This suggests a breakdown of the Nb₂O₅ film and exposure of the metallic matrix to wear. Figure 5b presents the results from the analysis after immersion in 0.9% NaCl solution. Here, a significant decrease in the variability of the COF values for the 316L SS (0.21) was observed. This reduction can be ascribed to the corrosion products formed on the sample surface, serving as a lubricant that diminishes the interaction between the Al₂O₃ sphere and the metallic surface [35]. Ferreira et al. [26] investigated the impact of Nb₂O₅ and carbon nanostructured coatings on the corrosion resistance of 316L SS when exposed to 0.6 mol L⁻¹ NaCl solution by using open circuit potential (OCP), potentiodynamic polarization curves (PPCs), and electrochemical impedance spectroscopy (EIS). The authors reported that these corrosion products are likely to seal the pits present on the surface. Otherwise, for the 316L SS/Nb₂O₅ sample, no statistical reduction of the COF values in comparison with the air condition is observed.

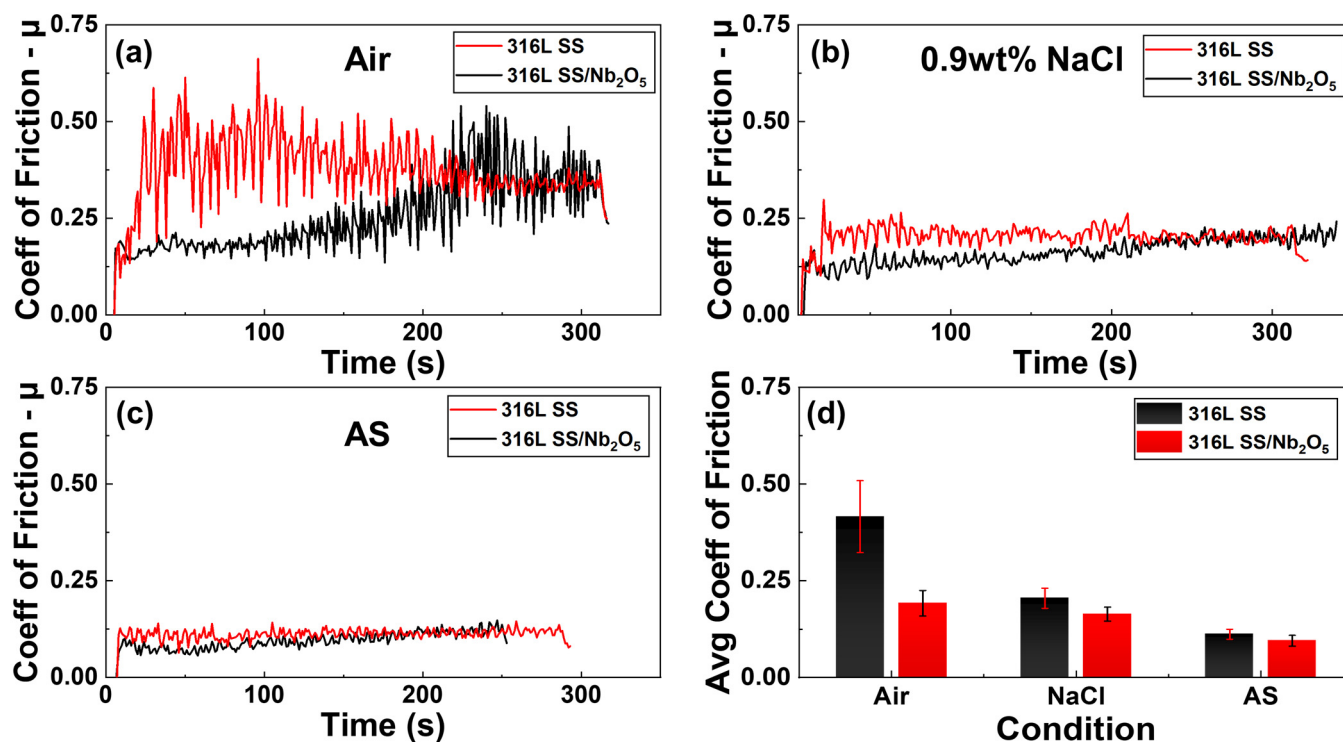


Figure 5. Coefficient of friction of 316L SS and 316L SS/Nb₂O₅ for different conditions: (a) air, (b) 0.9 wt% NaCl solution after 2 h of immersion, (c) AS after 2 h of immersion, and (d) comparison average COF for all the tested materials.

When examining the analyses of the samples post-immersion in AS, as shown in Figure 5c, a significant alteration in the COF values (0.11) and wear mechanism for the uncoated sample is observed. Moreto et al. [36], while studying the corrosion behaviour of the CoCrMo alloy in Hank's solution, observed an increase in the corrosion resistance of the alloy after 168 h of immersion. The authors attributed such counterintuitive behaviour to the formation of a D-glucose thin film due to the composition of the tested solution. In this context, a comparable phenomenon may be taking place with the AS solution, resulting in a decrease in the friction COF. Regarding the 316L SS/Nb₂O₅ specimen, this same effect could elucidate the decline in the COF (0.09), albeit to a lesser extent compared to the uncoated sample.

The CLSM analysis for the 316L SS and 316L SS/Nb₂O₅ after the pin-on-disk tests in the air condition may be seen in Figures 6a and 6d, respectively. Considering the 316L SS, the wear track exhibits parallel grooves that align with the direction of rotation of the disc, indicative of a two-body abrasive wear mechanism. This wear phenomenon arises from friction between two bodies possessing differing hardness values, such as 316L SS and the Al₂O₃ sphere used in the mechanical tests. Considering 316L SS/Nb₂O₅ tested in air, the greenish hue may be associated with the Nb₂O₅ coating deposited on the 316L SS surface by using the reactive sputtering technique, while the greyish region corresponds to the metallic substrate. These results are consistent with the data obtained for the COF, as the coated material showed an increase in its COF after 200 s, indicating failure of the Nb₂O₅ layer. However, upon comparing the CLSM images of the coated material with those of the substrate, the difference in dimensions becomes apparent. Consequently, it can be concluded that the Nb₂O₅ coating was effective in protecting the metallic substrate against wear processes, thereby contributing to an increased service life.

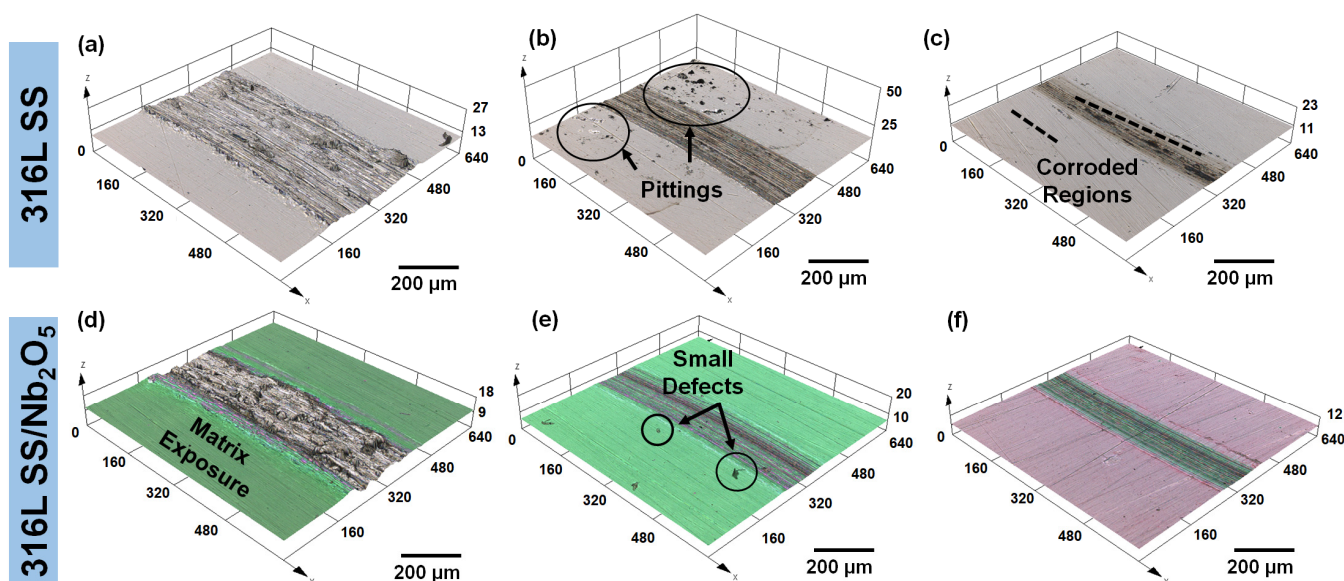


Figure 6. CLSM analysis for the 316L SS and 316L SS/Nb₂O₅ after the pin-on-disk tests: (a,d) air, (b,e) 0.9 wt% NaCl solution after 2 h of immersion, and (c,f) AS after 2 h of immersion. Magnification of 500×.

Figure 6b illustrates the wear track of 316L SS following exposure to 0.9% NaCl solution. This result not only reveals the same abrasive wear pattern observed under atmospheric conditions, but also highlights the presence of various pits scattered across its surface. These pits are likely the result of corrosion processes induced by the exposure of 316L SS to the corrosive environment. Pitting is a localised form of corrosion which can ultimately compromise structural integrity, and when the protective oxide layer on the metal is disrupted, permits aggressive ions, such as chlorides, to penetrate the underlying substrate. It is important to emphasise that the development and propagation of these pits are influenced by several factors, including the electrochemical properties of the metal, the presence of corrosive agents, and specific environmental conditions. The wear track exhibited smaller dimensions in this condition compared to that observed in air. This phenomenon can be attributed to the presence of corrosion products, which acted as mitigators of the wear process, as well as the development of a thicker oxide layer on the surface of 316L SS when exposed to an aggressive environmental condition [37,38].

Upon analysing the topography of the 316L/Nb₂O₅ after immersion in 0.9% NaCl solution, a drastic reduction in the wear profile is observed (see Figure 6e). Furthermore, it is evident that the process displays characteristics typical of two-body abrasive wear, likely arising from the difference in hardness between the Nb₂O₅ coating and the Al₂O₃ sphere. The reduction in wear under these conditions cannot be attributed to the formation of corrosion products, as the Nb₂O₅ coating has proven to be extremely effective in protecting the metallic substrate, even after prolonged exposure to highly aggressive solutions [26,29,31]. Figure 6c,f illustrates the wear results for the 316L SS and 316L SS/Nb₂O₅ samples following exposure to AS solution for 2 h. As shown, there was a reduction in the wear volume of these specimens when compared to the conditions of air and 0.9% NaCl solution. The most plausible explanation for the observed reduction in wear volume and COF is the formation of a D-glucose thin film on the surface of the studied samples [36]. Alongside acquiring the wear track via confocal microscopy, comprehensive data about the worn area of the specimens under each analysed condition were obtained. Four cross-section regions of the wear track were verified, yielding 12 measurements for the present study. Following this, the mean of all values generated by the equipment's software was calculated in conjunction with the diameters of each wear track, as shown in Figure 7.

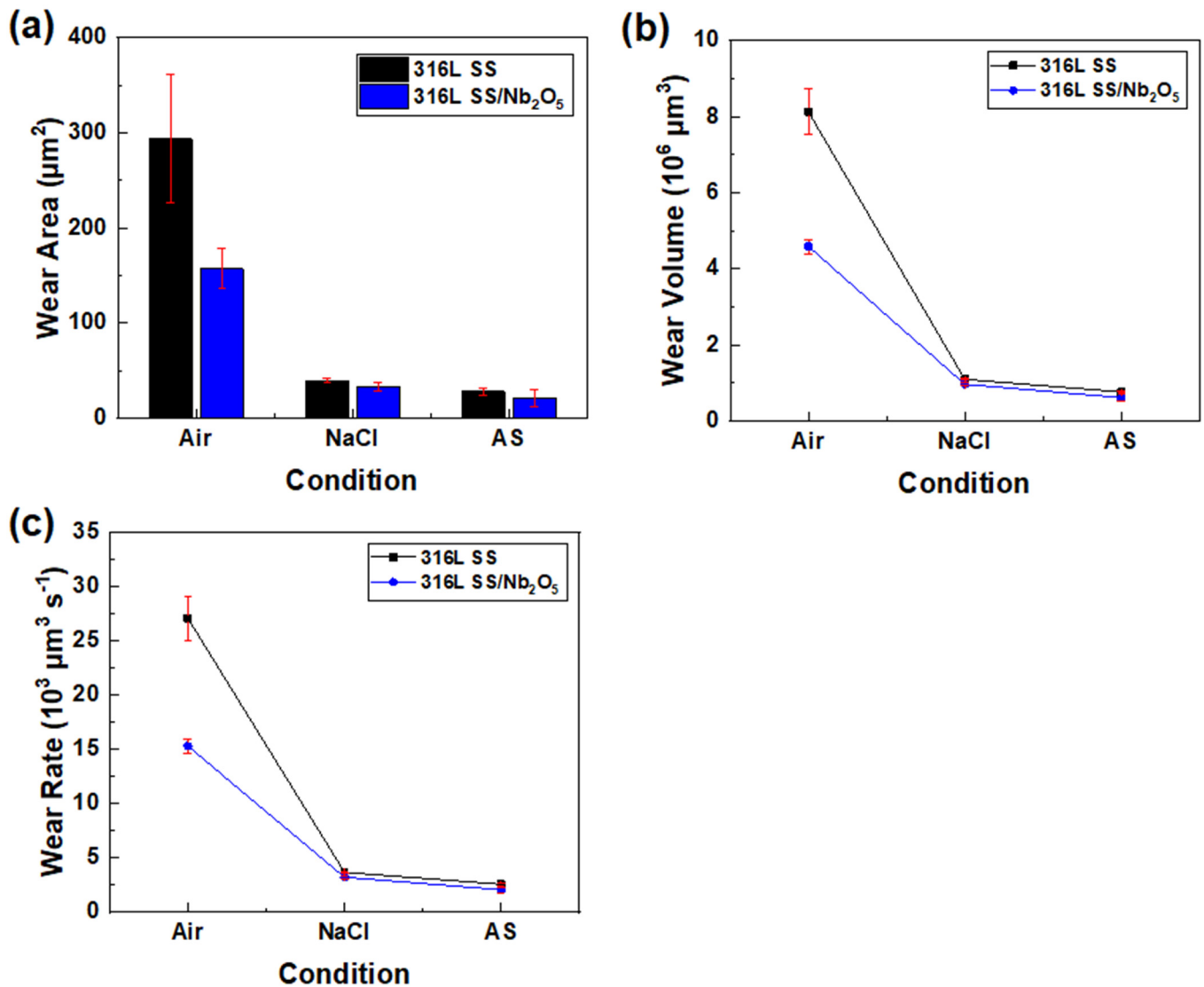


Figure 7. Summary of wear results for 316L SS and 316L SS/Nb₂O₅ tested under different conditions: (a) wear area, (b) wear volume, and (c) wear rate.

Among all of the conditions studied, the tests conducted in air demonstrated the highest wear volumes. The Nb₂O₅ coating, in turn, resulted in a significant reduction in the amount of material removed, approximately 50% compared to the uncoated material. Furthermore, a notable decrease in wear volume values was observed for both 316L SS and 316L SS/Nb₂O₅ in the tests conducted following immersion in 0.9% NaCl and AS, respectively. This is likely associated with the corrosion products formed on the surface of the samples, which can act as mitigators in the wear process [38]. Moreover, another factor that may impact the wear of 316L SS is the high concentration of chromium (Cr). This element contributes to a thicker passive film on the material's surface, promoting a more rapid repassivation when immersed in an aggressive medium [37]. This, in turn, provides additional protection to the substrate against corrosion and wear processes with prolonged immersion time, a phenomenon documented by authors such as Ferreira et al. [26] and Labiapari et al. [37]. However, in the present study, only the performance of 316L SS after immersion was evaluated, rather than under tribocorrosion conditions, meaning that the effects of film repassivation on the substrate did not influence its wear performance.

Additionally, even considering a scenario in which the wear volume is significantly lower, the coated material exhibited lower values compared to the base material, indicating that the Nb₂O₅ coating produced by using the reactive sputtering technique reduced

the amount of material removed and, consequently, extended the wear life of 316L SS. Specifically for the 0.9% NaCl solution, the wear area found for 316L SS/Nb₂O₅ is 16.3% lower than that of the uncoated material. Concerning the 316L SS/Nb₂O₅ exposed to the AS solution, a reduction in the wear area of approximately 25% was observed. It is important to note that, following immersion in both media, only the Nb₂O₅ coating underwent wear, without any exposure of the metallic substrate, whereas the base material experienced wear directly within its metallic matrix. For the tests conducted in air, both the base material and the coated one displayed the highest COF values, indicating a greater interaction between the surfaces of these samples and the sphere used for the pin-on-disk tests, resulting in a larger volume of removed material. However, the COF for the 316L SS and 316L/Nb₂O₅ samples after exposure to 0.9% NaCl and AS solutions were lower in comparison to those in air. This, in turn, corresponds to reduced wear volumes due to the lesser interaction between the pin-on-disk sphere and the surfaces of the samples. Finally, this finding can be summarized in Figure 7c, which highlights the wear rate for all of the tested conditions, in which the Nb₂O₅ coatings were able to reduce the rate of material removal when compared to the uncoated 316L SS.

The SEM/EDX analysis of 316L SS following the pin-on-disk tests conducted under air conditions is presented in Figure 8a. The results indicated a strong interaction between the metallic substrate and the sphere during the tests. This is evident from the presence of cavities and irregularities at the centre of the wear track, as well as the grooving aligned with the direction of the pin's motion, which characterizes the wear type as abrasive. Similar wear track characteristics were observed in the study conducted by Alvi and colleagues [39], who investigated the influence of laser treatments on the wear behaviour of 316L SS. The authors identified abrasive markings on the wear track under all tested conditions, resembling those exhibited in the present work. They noted the presence of grooves and fine particles along the wear track; in line with the results obtained in the present study, Ralls et al. [40], Özer et al. [41], and Li et al. [20] reported analogous characteristics concerning the wear performance of 316L SS. EDX analysis showed the presence of iron (Fe), chromium (Cr), nickel (Ni), manganese (Mn), and oxygen (O) elements, which is expected given that the material is 316L SS. Figure 8b presents the SEM/EDX results corresponding to the 316L SS/Nb₂O₅ specimen tested in air. As previously discussed, the 316L SS/Nb₂O₅ sample exhibited a highly irregular profile in the wear track (see Figure 5d), which pertains to the external surface of the specimen, where the wear process is still in the establishment phase. This morphological difference is evident when comparing materials with and without Nb₂O₅ coating. The EDX maps confirmed the presence of Fe, Cr, Ni, O, and Nb elements. Figure 8c displays the SEM image regarding the 316L SS specimen exposed to 0.9% NaCl solution. A more clearly defined wear pattern can be observed compared to the 316L SS tested in air. In other words, there is not only a reduced number of regions with cavities, but also potential debris resulting from the wear process, and some corrosion products throughout the central part of the wear track. This hypothesis is supported by the EDX maps.

In relation to the 316L SS/Nb₂O₅ sample exposed to 0.9% NaCl solution (Figure 8d), the presence of delamination regions in the wear track was observed. This finding was corroborated by the increased concentration of Fe and Ni elements in isolated points, as demonstrated by the EDX maps. Regarding the 316L SS specimens subjected to the AS solution (see Figure 8e), parallel lines are observed on the wear track, indicating a more pronounced degradation process. This area exhibits various corrosion products, which is supported by the high concentration of oxygen distributed across its surface, as shown in the EDX map. Furthermore, several cavities are present in this region, although they are found in significantly lower quantities compared to the 316L SS specimens exposed to air. Finally, considering the 316L SS/Nb₂O₅ exposed to AS solution (Figure 8f), it is evident that the coating produced by the reactive sputtering technique remained intact and did not exhibit delamination, in contrast to the observations made following immersion in the 0.9%

NaCl solution. Figure 9 presents the profilometry analysis of a segment from both 316L SS and 316L SS/Nb₂O₅, showing the wear track topography.

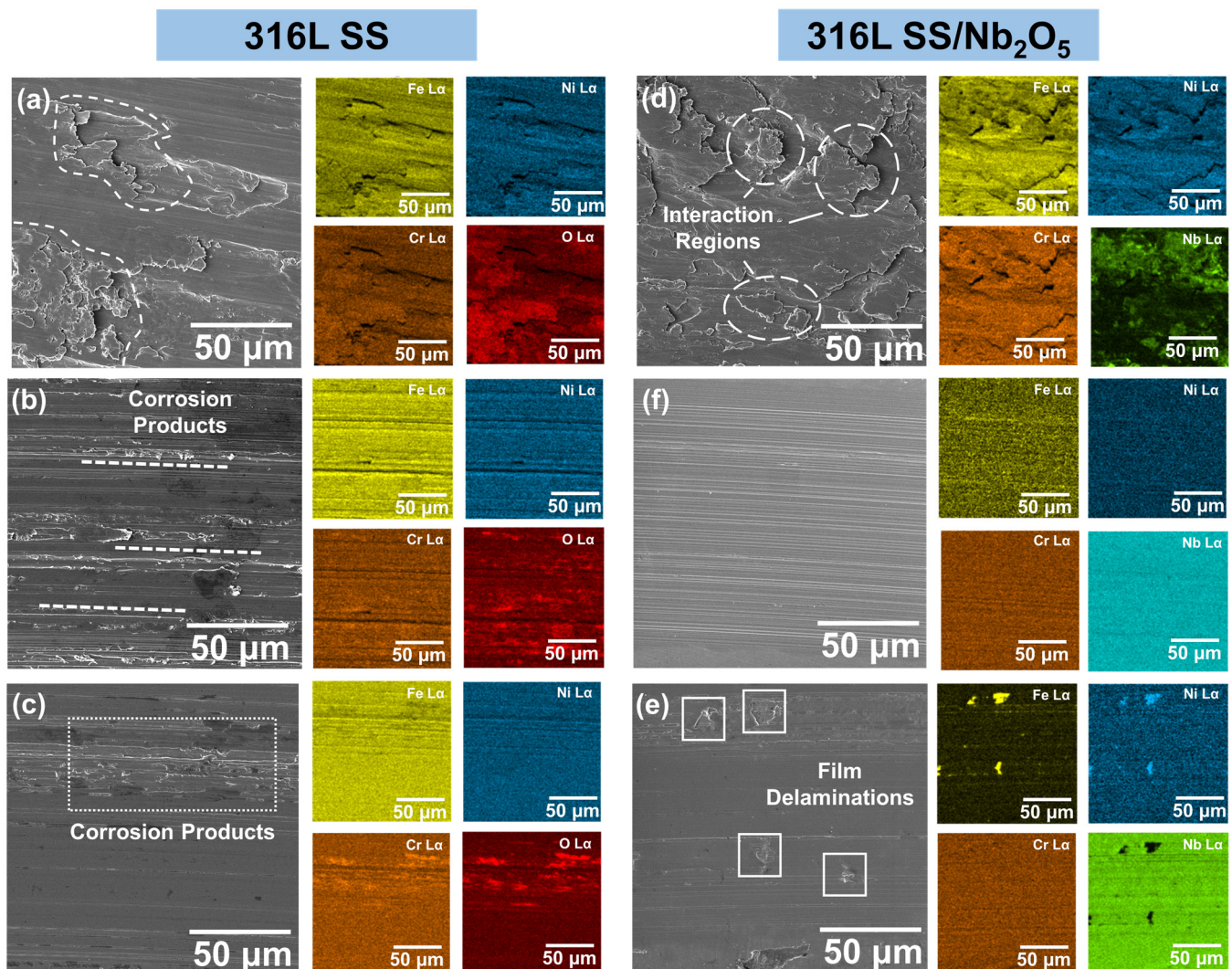


Figure 8. SEM/EDX analysis for the 316L SS and 316L SS/Nb₂O₅ after the pin-on-disk tests in (a,d) air, (b,e) 0.9 wt% NaCl solution after 2 h of immersion, and (c,f) AS after 2 h of immersion.

The results reveal a non-uniform wear track profile characterised by multiple grooves in both samples, which is consistent with the findings from the CLSM and SEM/EDX analyses. As previously discussed, these grooves are attributable to the high level of interaction between the uncoated sample surface and the Al₂O₃ sphere. In contrast, the coated 316L SS exhibits a more uniform profile with a shallower wear track, likely attributed to the higher hardness of the coating, which reduces interaction with the Al₂O₃ sphere (see Figure 10). Furthermore, changes in environmental conditions affect the wear track depth in both uncoated and coated samples. This variation corresponds to the wear mechanisms previously discussed for the NaCl solution and AS. After immersion in 0.9 wt% NaCl solution, the corrosion products on 316L SS and surface deposition of NaCl on 316L SS/Nb₂O₅ reduce the coefficient of friction, lowering the interaction between the sphere and the sample surfaces during pin-on-disk tests. This reduction is accompanied by less variation in wear track depth in both samples. For samples immersed in AS, the D-glucose thin film reduced the interaction between the sphere and the material surfaces. However, despite a slightly lower wear track depth, the 316L SS sample exhibited significantly greater

variation in values compared to 316L SS/Nb₂O₅, indicating that the D-glucose thin film did not protect the 316L SS surface against wear as effectively as Nb₂O₅.

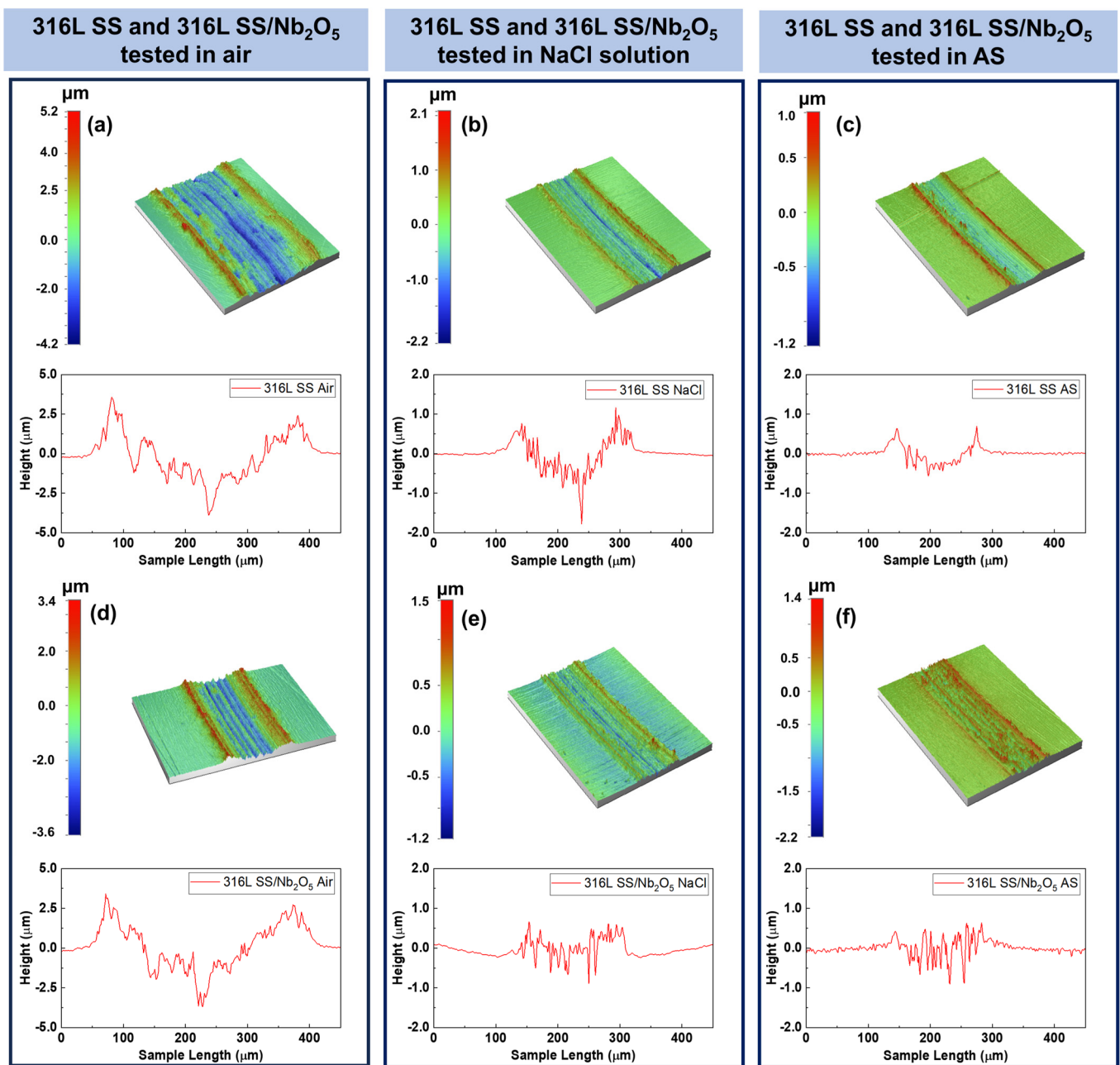


Figure 9. Profilometry analysis and respective wear track profile for the 316L SS and 316L SS/Nb₂O₅ in (a,d) air, (b,e) after immersion in 0.9 wt% NaCl solution, and (c,f) after immersion in AS.

Figure 11 displays a schematic representation of the wear mechanism for 316L SS and 316L SS/Nb₂O₅ under the different tested environmental conditions. Here, it is possible to verify that in air, only the interaction of the Al₂O₃ sphere and the sample surfaces affected the removal of material. Thus, it can be observed that a harder surface exhibited a lower volume of material removal. When considering the samples after immersion in 0.9 wt% NaCl solution, several corrosion products and deposited particles were present, which acted as lubricants, thereby reducing the interaction between the sphere and the metallic substrate. Finally, the samples immersed in AS displayed the distinctive formation of a D-glucose thin film that partially protected the surface against wear.

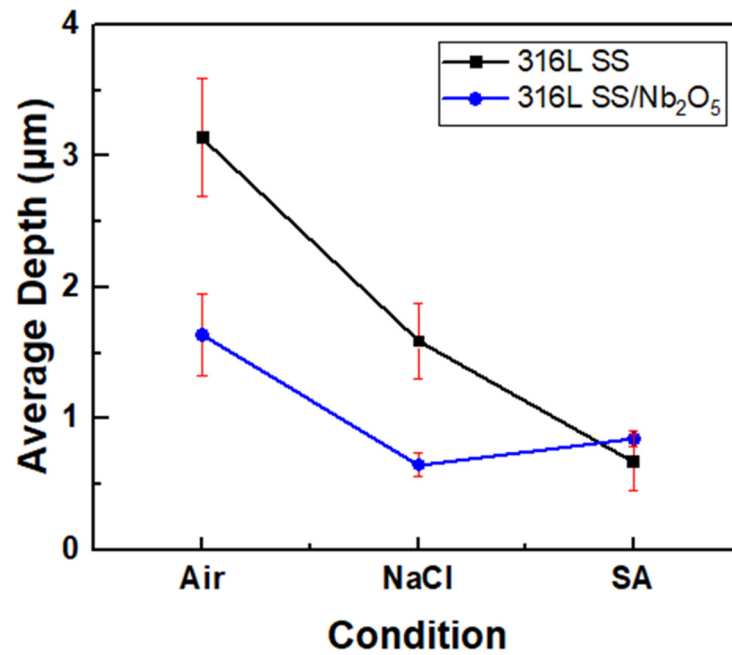


Figure 10. Average depth of the wear track for the 316L SS and 316L SS/ Nb_2O_5 under different environmental conditions.

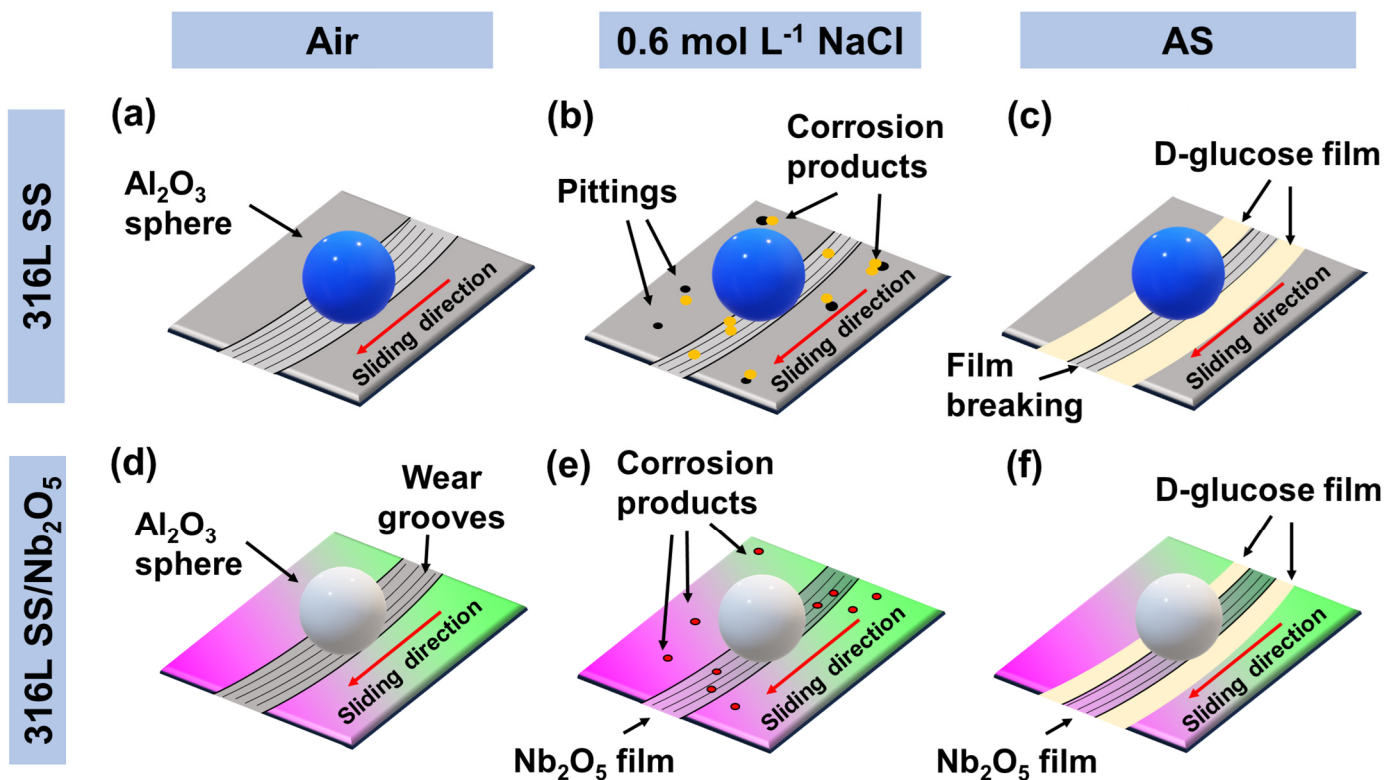


Figure 11. A schematic representation illustrating the influence of environmental conditions on the wear performance of 316L SS and 316L SS/ Nb_2O_5 in (a,d) air, (b,e) after immersion in 0.9 wt% NaCl solution, and (c,f) after immersion in AS.

4. Conclusions

The pin-on-disk analysis revealed that environmental conditions prominently influenced the wear behaviour of both the 316L SS and the 316L SS/ Nb_2O_5 specimens. Notably, among all of the samples tested, those exposed to air displayed the highest wear volume,

as these conditions were devoid of interfering compounds, such as corrosion products or thin saccharide films, which can mitigate wear. In contrast, the Nb₂O₅ coating emerged as a highly effective solution for enhancing the wear properties of 316L SS. The presence of this coating not only led to a significant reduction in the coefficient of friction, but also decreased the wear area substantially, even after extended exposure to adverse conditions. This enhancement in wear performance underscores the potential of Nb₂O₅ coatings in extending the lifespan of biomedical implants and other applications where wear resistance is critical.

Author Contributions: Investigation, M.O.A.F., V.A.F.M., K.R.d.S., F.E.M., R.V.G., M.M.M., R.G.J. and C.A.F.; formal analysis, M.O.A.F., N.B.L.S., C.A.F., R.G.J., H.C.P., R.V.G., R.G. and J.A.M.; writing, M.O.A.F. and J.A.M.; project administration, J.A.M. All authors have read and agreed to the published version of the manuscript.

Funding: This research was funded by the National Council for Scientific and Technological Development (CNPq-Brazil), the Foundation for Research Support of the State of Minas Gerais (FAPEMIG-Brazil), Coordination for the Improvement of Higher Education Personnel (CAPES-Brazil) and São Paulo Research Foundation (FAPESP).

Data Availability Statement: Not applicable.

Acknowledgments: J.A.M would like to acknowledge the financial support received from the National Council for Scientific and Technological Development (CNPq-Brazil) (Grants 303659/2019-0, 402988/2021-3, 302770/2022-4). N.B.L.S would like to acknowledge the financial support received from the Foundation for Research Support of the State of Minas Gerais (FAPEMIG-Brazil) (Process: APQ-00554-21). R.V.G thanks the CNPq, the Minas Gerais Research Foundation (CNPq 302582/2021-5 and FAPEMIG APQ-01359-21), and Companhia Brasileira de Metalurgia e Mineração (CBMM) for the Nb donation. The author M.O.A.F thanks the Coordination for the Improvement of Higher Education Personnel (CAPES-Brazil) for the master's scholarship. M.M.M would like to thank the scholarship grant 2020/16012-1, São Paulo Research Foundation (FAPESP). R.G. would like to thank the scholarship grant 2022/07162,5, São Paulo Research Foundation (FAPESP).

Conflicts of Interest: The authors declare that they have no known competing financial interests or personal relationships that could have appeared to influence the work reported in this paper.

References

1. Bohara, S.; Suthakorn, J. Surface Coating of Orthopedic Implant to Enhance the Osseointegration and Reduction of Bacterial Colonization: A Review. *Biomater. Res.* **2022**, *26*, 26. [\[CrossRef\]](#)
2. Humphreys, H. Surgical Site Infection, Ultraclean Ventilated Operating Theatres and Prosthetic Joint Surgery: Where Now? *J. Hosp. Infect.* **2012**, *81*, 71–72. [\[CrossRef\]](#)
3. Ruggiero, A.; De Stefano, M. Experimental Investigation on the Bio-Tribocorrosive Behavior of Ti-6Al-4V Alloy and 316L Stainless Steel in Two Biological Solutions. *Tribol. Int.* **2023**, *190*, 109033. [\[CrossRef\]](#)
4. Hatem, A.; Lin, J.; Wei, R.; Torres, R.D.; Laurindo, C.; Soares, P. Tribocorrosion Behavior of DLC-Coated Ti-6Al-4V Alloy Deposited by PIIID and PEMS + PIIID Techniques for Biomedical Applications. *Surf. Coat. Technol.* **2017**, *332*, 223–232. [\[CrossRef\]](#)
5. Mi, B.; Wang, H.; Wang, Q.; Cai, J.; Qin, Z.; Chen, Z. Corrosion Resistance and Contact Resistance Properties of Cr-Doped Amorphous Carbon Films Deposited under Different Carbon Target Current on the 316L Stainless Steel Bipolar Plate for PEMFC. *Vacuum* **2022**, *203*, 111263. [\[CrossRef\]](#)
6. Kazemi, M.; Ahangarani, S.; Esmailian, M.; Shanaghi, A. Investigating the Corrosion Performance of Ti-6Al-4V Biomaterial Alloy with Hydroxyapatite Coating by Artificial Neural Network. *Mater. Sci. Eng. B* **2022**, *278*, 115644. [\[CrossRef\]](#)
7. Vazirian, S.; Farzadi, A.; Solouk, A. Joining Dental Biomaterials of Ti-6Al-4V Alloy and Cp-Ti Using Transient Liquid Phase Bonding: Metallurgical and Mechanical Assessment. *Mater. Today Commun.* **2022**, *32*, 103981. [\[CrossRef\]](#)
8. Anees, E.; Riaz, M.; Hussain, T. Electrochemical Corrosion Study of CH-xTiO₂ (x=Ag, Mg, Sr, and Zn) Coated Ti-6Al-4V Alloy for Dental Implant. *Mater. Chem. Phys.* **2024**, *327*, 129895. [\[CrossRef\]](#)
9. Bernal-Alvarez, L.R.; Ramirez-Gutierrez, C.F.; Gomez-Vazquez, O.M.; Correa-Piña, B.A.; Zubieta-Otero, L.F.; Millán-Malo, B.M.; Rodriguez-Garcia, M.E. Enhancing Surface Chemistry and Wetting Behavior of Laser-Modified Ti-6Al-4V Surgical Titanium Alloy Surfaces through Wet Deposition of Biogenic Hydroxyapatite. *Surf. Coat. Technol.* **2024**, *489*, 131065. [\[CrossRef\]](#)
10. Wei, G.; Tan, M.; Attarilar, S.; Li, J.; Uglov, V.V.; Wang, B.; Liu, J.; Lu, L.; Wang, L. An Overview of Surface Modification, A Way toward Fabrication of Nascent Biomedical Ti-6Al-4V Alloys. *J. Mater. Res. Technol.* **2023**, *24*, 5896–5921. [\[CrossRef\]](#)

11. Demirci, S.; Dalmuş, R.; Dikici, T.; Tünçay, M.M.; Kaya, N.; Güllüoğlu, A.N. Effect of Surface Modifications of Additively Manufactured Ti-6Al-4V Alloys on Apatite Formation Ability for Biomedical Applications. *J. Alloys Compd.* **2021**, *887*, 161445. [[CrossRef](#)]
12. Romero-Resendiz, L.; Rossi, M.C.; Álvarez, A.; García-García, A.; Milián, L.; Tormo-Más, M.Á.; Amigó-Borrás, V. Microstructural, Mechanical, Electrochemical, and Biological Studies of an Electron Beam Melted Ti-6Al-4V Alloy. *Mater. Today Commun.* **2022**, *31*, 103337. [[CrossRef](#)]
13. Nisar, S.S.; Choe, H.-C. Mechanical Hydroxyapatite Coatings on PEO-Treated Ti-6Al-4V Alloy for Enhancing Implant's Surface Bioactivity. *Ceram. Int.* **2024**, *50*, 17703–17719. [[CrossRef](#)]
14. Praveenkumar, K.; Vishnu, J.; Raheem, A.; Gopal, V.; Swaroop, S.; Suwas, S.; Shankar, B.; Manivasagam, G. In-Vitro Fretting Tribocorrosion and Biocompatibility Aspects of Laser Shock Peened Ti-6Al-4V Surfaces. *Appl. Surf. Sci.* **2024**, *665*, 160334. [[CrossRef](#)]
15. Mahlobo, M.G.R.; Chikosha, L.; Olubambi, P.A. Study of the Corrosion Properties of Powder Rolled Ti-6Al-4V Alloy Applied in the Biomedical Implants. *J. Mater. Res. Technol.* **2022**, *18*, 3631–3639. [[CrossRef](#)]
16. Pathote, D.; Jaiswal, D.; Singh, V.; Behera, C.K. Optimization of Electrochemical Corrosion Behavior of 316L Stainless Steel as an Effective Biomaterial for Orthopedic Applications. *Mater. Today Proc.* **2022**, *57*, 265–269. [[CrossRef](#)]
17. Parau, A.C.; Juravlea, G.A.; Raczkowska, J.; Vitelaru, C.; Dinu, M.; Awsiuk, K.; Vranceanu, D.M.; Ungureanu, E.; Cotrut, C.M.; Vladescu, A. Comparison of 316L and Ti-6Al-4V Biomaterial Coated by ZrCu-Based Thin Films Metallic Glasses: Structure, Morphology, Wettability, Protein Adsorption, Corrosion Resistance, Biomineralization. *Appl. Surf. Sci.* **2023**, *612*, 155800. [[CrossRef](#)]
18. Danish, M.; Al-Amin, M.; Rubaiee, S.; Gul, I.A.; Ahmed, A.; Rahman, M.O.; Zhang, C.; Yildirim, M.B. Investigation of Coated 316L Steel Surface: Surface Morphology, Composition, Corrosion, and Biocompatibility Using Hydroxyapatite Mixed-EDM Process. *Surf. Coat. Technol.* **2023**, *467*, 129689. [[CrossRef](#)]
19. Pandey, A.K.; Kumar, A.; Kumar, R.; Gautam, R.K.; Behera, C.K. Tribological Performance of SS 316L, Commercially Pure Titanium, and Ti-6Al-4V in Different Solutions for Biomedical Applications. *Mater. Today Proc.* **2023**, *78*, A1–A8. [[CrossRef](#)]
20. Li, J.; Zhang, X.; He, X.; Hang, R.; Huang, X.; Tang, B. Preparation, Biocompatibility and Wear Resistance of Microstructured Zr and ZrO₂ Alloyed Layers on 316L Stainless Steel. *Mater. Lett.* **2017**, *203*, 24–27. [[CrossRef](#)]
21. Atmaca, I.; Dikici, B.; Ezirmik, K.V.; Gunay Bulutsuz, A.; Niinomi, M. Investigation of Corrosion and Wear Performance of TiNbTaZr/Cr-Mo PVD Coatings on 316L SS in Hanks's Solution for Improved Biomedical Applications. *Surf. Coat. Technol.* **2023**, *473*, 130021. [[CrossRef](#)]
22. Katta, P.P.; Nalliyar, R. Corrosion Resistance with Self-Healing Behavior and Biocompatibility of Ce Incorporated Niobium Oxide Coated 316L SS for Orthopedic Applications. *Surf. Coat. Technol.* **2019**, *375*, 715–726. [[CrossRef](#)]
23. PremKumar, K.P.; Durairandy, N.; Kiran, M.S.; Rajendran, N. Antibacterial Effects, Biocompatibility and Electrochemical Behavior of Zinc Incorporated Niobium Oxide Coating on 316L SS for Biomedical Applications. *Appl. Surf. Sci.* **2018**, *427*, 1166–1181. [[CrossRef](#)]
24. Dincel, Ö.; Şimşek, İ.; Özyürek, D. Investigation of the Wear Behavior in Simulated Body Fluid of 316L Stainless Steels Produced by Mechanical Alloying Method. *Eng. Sci. Technol. Int. J.* **2021**, *24*, 35–40. [[CrossRef](#)]
25. Wongpanya, P.; Wongpinij, T.; Photongkam, P.; Siritapetawee, J. Improvement in Corrosion Resistance of 316L Stainless Steel in Simulated Body Fluid Mixed with Antiplatelet Drugs by Coating with Ti-Doped DLC Films for Application in Biomaterials. *Corros. Sci.* **2022**, *208*, 110611. [[CrossRef](#)]
26. Ferreira, M.O.A.; Mariani, F.E.; Leite, N.B.; Gelamo, R.V.; Aoki, I.V.; De Siervo, A.; Pinto, H.C.; Moreto, J.A. Niobium and Carbon Nanostructured Coatings for Corrosion Protection of the 316L Stainless Steel. *Mater. Chem. Phys.* **2024**, *312*, 128610. [[CrossRef](#)]
27. Moreto, J.A.; Gelamo, R.V.; Da Silva, M.V.; Steffen, T.T.; De Oliveira, C.J.F.; De Almeida Buranello, P.A.; Pinto, M.R. New Insights of Nb₂O₅-Based Coatings on the 316L SS Surfaces: Enhanced Biological Responses. *J. Mater. Sci. Mater. Med.* **2021**, *32*, 25. [[CrossRef](#)]
28. Davis, J.R. (Ed.) *ASM Specialty Handbook: Stainless Steels*; ASM International: West Conshohocken, PA, USA, 1994; Volume 518.
29. Nascimento, J.P.L.; Teixeira, G.T.L.; Obata, M.M.S.; Silva, M.V.; Oliveira, C.J.F.; Silva, L.E.A.; Gelamo, R.V.; Slade, N.B.L.; Moreto, J.A. Influence of Reactive Sputtering-Deposited Nb₂O₅ Coating on the Ti-6Al-4V Alloy Surfaces: Biomineralization, Antibacterial Activity, and Cell Viability Tests. *Mater. Res.* **2023**, *26*, e20230251. [[CrossRef](#)]
30. Silva, T.I.; Ferreira, M.O.A.; Nascimento, J.P.L.; Pietro, L.R.; Neto, L.A.R.C.; Moreira, H.C.; Pereira, L.V.; Leite, N.B.S.; Gelamo, R.V.; Moreto, J.A. Development of a Low-Cost Ball-on-Flat Linear Reciprocating Apparatus: Test Validation Using Ti-6Al-4V and Ti-6Al-4V/Nb₂O₅ Coatings. *J. Mater. Sci. Technol. Res.* **2022**, *9*, 43–52. [[CrossRef](#)]
31. Nascimento, J.P.L.; Ferreira, M.O.A.; Gelamo, R.V.; Scarmínio, J.; Steffen, T.T.; Da Silva, B.P.; Aoki, I.V.; dos Santos, A.G., Jr.; De Castro, V.V.; Malfatti, C.F.; et al. Enhancing the Corrosion Protection of Ti-6Al-4V Alloy through Reactive Sputtering Niobium Oxide Thin Films. *Surf. Coat. Technol.* **2021**, *428*, 127854. [[CrossRef](#)]
32. Gelamo, R.V.; Slade, N.B.L.; Amadeu, N.; Tavares, M.R.P.M.; Oberschmidt, D.; Klemm, S.; Fleck, C.; Cakir, C.-T.; Radtke, M.; Moreto, J.A. Exploring the Nb₂O₅ Coating Deposited on the Ti-6Al-4V Alloy by a Novel GE-XANES Technique and Nanoindentation Load-Depth. *Mater. Lett.* **2024**, *355*, 135584. [[CrossRef](#)]
33. ASTM G99-23; Standard Test Method for Wear and Friction Testing with a Pin-on-Disk or Ball-on-Disk Apparatus. ASTM International: West Conshohocken, PA, USA, 2017. [[CrossRef](#)]

34. García-León, R.A.; Martínez-Trinidad, J.; Zepeda-Bautista, R.; Campos-Silva, I.; Guevara-Morales, A.; Martínez-Londoño, J.; Barbosa-Saldaña, J. Dry Sliding Wear Test on Borided AISI 316L Stainless Steel under Ball-on-Flat Configuration: A Statistical Analysis. *Tribol. Int.* **2021**, *157*, 106885. [[CrossRef](#)]
35. Ma, X.; Tan, W.; Bonzom, R.; Mi, X.; Zhu, G. Impact-Sliding Fretting Tribocorrosion Behavior of 316L Stainless Steel in Solution with Different Halide Concentrations. *Friction* **2023**, *11*, 2310–2328. [[CrossRef](#)]
36. Moreto, J.A.; Rodrigues, A.C.; Leite, R.R.D.S.; Rossi, A.; Silva, L.A.D.; Alves, V.A. Effect of Temperature, Electrolyte Composition and Immersion Time on the Electrochemical Corrosion Behavior of CoCrMo Implant Alloy Exposed to Physiological Serum and Hank's Solution. *Mater. Res.* **2018**, *21*, e20170659. [[CrossRef](#)]
37. Labiapari, W.S.; Ardila, M.A.N.; Costa, H.L.; De Mello, J.D.B. Micro Abrasion-Corrosion of Ferritic Stainless Steels. *Wear* **2017**, *376–377*, 1298–1306. [[CrossRef](#)]
38. Alkan, S.; Gök, M.S. Effect of Sliding Wear and Electrochemical Potential on Tribocorrosion Behaviour of AISI 316 Stainless Steel in Seawater. *Eng. Sci. Technol. Int. J.* **2021**, *24*, 524–532. [[CrossRef](#)]
39. Alvi, S.; Saeidi, K.; Akhtar, F. High Temperature Tribology and Wear of Selective Laser Melted (SLM) 316L Stainless Steel. *Wear* **2020**, *448–449*, 203228. [[CrossRef](#)]
40. Ralls, A.M.; Daroonparvar, M.; Kasar, A.K.; Misra, M.; Menezes, P.L. Influence of Friction Stir Processing on the Friction, Wear and Corrosion Mechanisms of Solid-State Additively Manufactured 316L Duplex Stainless Steel. *Tribol. Int.* **2023**, *178*, 108033. [[CrossRef](#)]
41. Özer, G.; Kisasöz, A. The Role of Heat Treatments on Wear Behaviour of 316L Stainless Steel Produced by Additive Manufacturing. *Mater. Lett.* **2022**, *327*, 133014. [[CrossRef](#)]

Disclaimer/Publisher's Note: The statements, opinions and data contained in all publications are solely those of the individual author(s) and contributor(s) and not of MDPI and/or the editor(s). MDPI and/or the editor(s) disclaim responsibility for any injury to people or property resulting from any ideas, methods, instructions or products referred to in the content.